Available online at www.sciencedirect.com
ScienceDirect
Energy Reports 7 (2021) 140–149
www.elsevier.com/locate/egyr

The 17th International Symposium on District Heating and Cooling, Nottingham Trent University, 2021, 6–9 September, Nottingham, United Kingdom

Monitoring and aggregate modelling of an existing neutral temperature district heating network

Selva Calixto[a,b,*], Cenker Köseoğlu[b,c], Marco Cozzini[b], Giampaolo Manzolini[a]

[a] Department of Energy, Politecnico di Milano, Via Lambruschini 4, 20156 Milano, Italy
[b] Eurac Research, Institute for Renewable Energy, Viale Druso 1, 39100 Bolzano, Italy
[c] Free University of Bozen, Piazza Università, 1, 39100 Bolzano, Italy

Received 5 August 2021; accepted 22 August 2021

Abstract

This contribution provides preliminary modelling results and data analysis of an existing neutral-temperature district heating (NTDH) network. The word "neutral" in this context refers to the fact that the distribution temperature is close to the ambient temperature (e.g., 15–20 °C). This type of network is coupled with decentralized heat pumps (HP), for both heating and cooling. They offer the advantage of being reversible and the possibility of integrating low-temperature waste heat. The considered case is located in Ospitaletto, Italy. The network includes two sources (industrial waste heat at about 25 °C and ground source heat from aquifer wells at about 15 °C), it is mainly built with non-insulated pipes and has a length of approximately 2 km. Decentralized HPs installed at user substations provide the proper temperature for space heating and sanitary hot water production.

An approximate model was applied to analyse the network operation. This model is focused on energy balances aggregating all users as a lumped demand and explicitly includes the behaviour of HPs substations, a component not available in other district heating analysis tools. The simulation of an entire year of operation is considered, with an hourly resolution. Thermal load profiles are known and used as input to the model, while the outputs are compared with real data -a combination of weekly and hourly measurements at the users substations-which include annual heat supply, electricity consumptions, thermal losses, and seasonal performance factor (SPF). The results yield an overall deviation of 15% in the main indicators when using pre-defined data. In conclusion, even though the measured SPF is slightly lower than expected, the model reaches a reasonable agreement.
© 2021 The Author(s). Published by Elsevier Ltd. This is an open access article under the CC BY-NC-ND license (http://creativecommons.org/licenses/by-nc-nd/4.0/).

Peer-review under responsibility of the scientific committee of the 17th International Symposium on District Heating and Cooling, Nottingham Trent University, 2021.

Keywords: District heating and cooling; Heat pumps; Waste heat; Ground source; Energy modelling

* Corresponding author at: Department of Energy, Politecnico di Milano, Via Lambruschini 4, 20156 Milano, Italy.
E-mail address: selva.calixto@polimi.it (S. Calixto).

https://doi.org/10.1016/j.egyr.2021.08.162
2352-4847/© 2021 The Author(s). Published by Elsevier Ltd. This is an open access article under the CC BY-NC-ND license (http://creativecommons.org/licenses/by-nc-nd/4.0/).

Peer-review under responsibility of the scientific committee of the 17th International Symposium on District Heating and Cooling, Nottingham Trent University, 2021.

1. Introduction

One of the biggest challenges of conventional district heating (DH) systems is their high-temperature operation (80 °C or higher). As a result, distributed losses can be of the order of 10 to 30% on an annual basis, limiting the system's overall efficiency, and reducing the possibility to utilize renewable heat and exploit low-temperature waste heat sources [1]. Thus, there has been growing interest in decreasing the operating temperature, as emphasized in fourth-generation DH (4GDH) [2–4], in which the network temperature can be lowered for the direct production of space heating (SH) while sanitary hot water (SHW) preparation is sometimes considered with booster heat pumps (HPs) [5].

The neutral-temperature network with booster HPs concept (NT-DHC) proposes operating temperatures that are lowered in the range of 10–25 °C. Due to the recent and innovative nature of NT-DHC networks, a particular aspect that is commonly missing in current literature is the ability to model its performance, not only because the existing models do not focus on the analysis of decentralized HPs, but also because experimental data are scarce. Therefore, the aim of this contribution is twofold: to analyse the operation of a real NT-DHC network and to calibrate a lumped model suited to perform scenario analyses.

Design-oriented DH tools are highly technical and provide features for accurate operation management, but can be computationally very expensive, and in specific applications they can present a lack of transferability of the methods for wider usage. Exemplars of this kind are TERMIS [6], Thermos [7], and PlanHeat [8]. On the other hand, high-level modelling tools simulate the energy performance at a systemic level, with a low time-resolution as they are focused on the long-term planning, and typically miss the evaluation of relevant aspects in DH: thermal losses, electric energy consumed by the network pumps, substations efficiency, among others. Tools that fit in this category are EnergyPLAN [9], LEAP [10], Crystal City [11], and METIS [12].

The model described in this paper contributes to fill this gap. It is expected to be integrated into a larger framework, the purpose of which is to perform techno-economic and environmental expansion scenarios of future NT-DHC at the local/community level. To meet this goal, the pre-design support tool developed during the Flexynets project [13] was taken as a starting point. It preserves the lumped demand approach, the possibility to customize several pre-defined parameters, and quantifies the economic and environmental impact of various network configurations although these aspects are not discussed in this paper. The status of the NT-DHC network analysed in this case study comprises a small number of users, but an expansion is planned. In this version, a Python model is presented to fully analyse on an hourly basis its performance, thus a technical validation is carried out in this work.

2. Case study

2.1. Description of the considered network

The Ospitaletto network is a small DH system located in the north of Italy. It matches well the NT-DHC concept, being supplied by two low-temperature sources: industrial waste heat (WH) and aquifer wells at about 25 °C and 15 °C, respectively. Users are mainly schools, all endowed with HP substations, which raise the temperature level to about 55 °C, with fluctuations depending on the balance between SH and SHW production. The network has an extension of around 2 km, with a simple tree structure and a conventional 2-pipe system. The layout is shown in Fig. 1 (left panel), along with the location of the users and sources. A centralized pumping station located in the proximity of the aquifer wells performs the circulation. The network is primarily made with high-density polyethylene (HDPE) pipes without insulation, but part of the final distribution includes pre-insulated steel pipes. Considering the network's control logic, the main pump aims to keep a constant differential pressure in the user loop, meanwhile, regulation valves in the user substations provide a constant temperature difference (ΔT) of about 5 K. According to the operational plan of the network, only one of the sources is active at a time. The waste heat source (s_1) is known to be operating from Tuesday at 08:00 until Saturday at 16:00 every week except for national holidays, and the rest of the time is covered by the ground source (s_2). The temperature distribution of the two sources for a typical winter week is shown in the right panel of Fig. 1, in agreement with the nominal values mentioned above. The network operation started in the Fall of 2018.

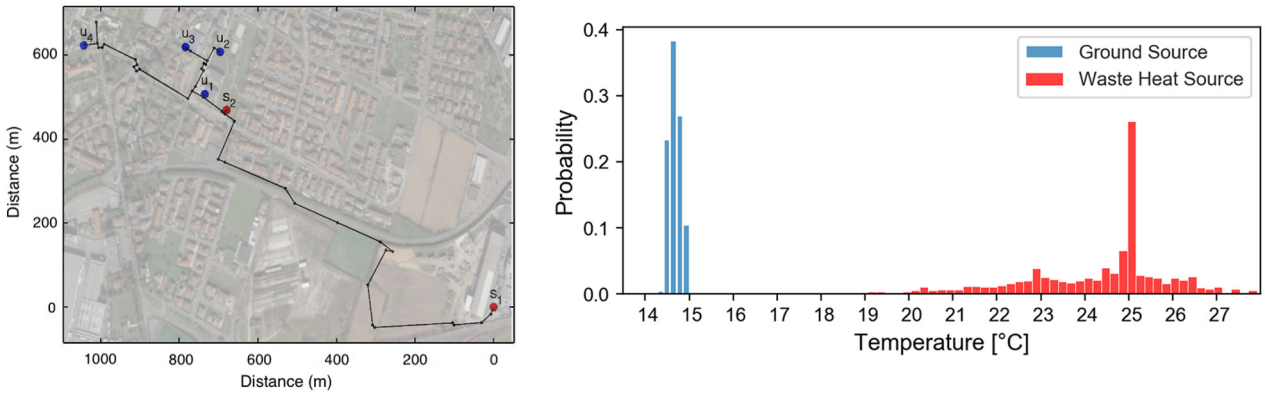

Fig. 1. (a) Network layout. Red and blue circles indicate sources (s_1, corresponding to the waste heat, and s_2, corresponding to the aquifer wells) and users ($u_1, \ldots, u_4$), respectively. Distances are measured from the source s1; (b) Probability histogram of sources temperatures in the period from Jan 13th to March 15th of 2020. (For interpretation of the references to colour in this figure legend, the reader is referred to the web version of this article.)

2.2. Data analysis of the network operation

Different sets of data were made available by the network manager (from the COGEME company). For 2019, weekly or biweekly monitoring data included all the main energy measurements (user thermal consumptions, HPs electricity, and network pumping consumptions). Hourly data for 2020 also included specific measurements (temperatures and flow rates at different points of the network). Unfortunately, due to the Covid-19 emergency, the overall operation of 2020 is far from being representative (schools were closed from early March until the reopening in September). Hence, to analyse the overall network performance a mixed approach was used: the yearly performance analysis was based on 2019 data, while the detailed analysis of single aspects (e.g., daily profiles and thermal losses) was carried out using selected 2020 data.

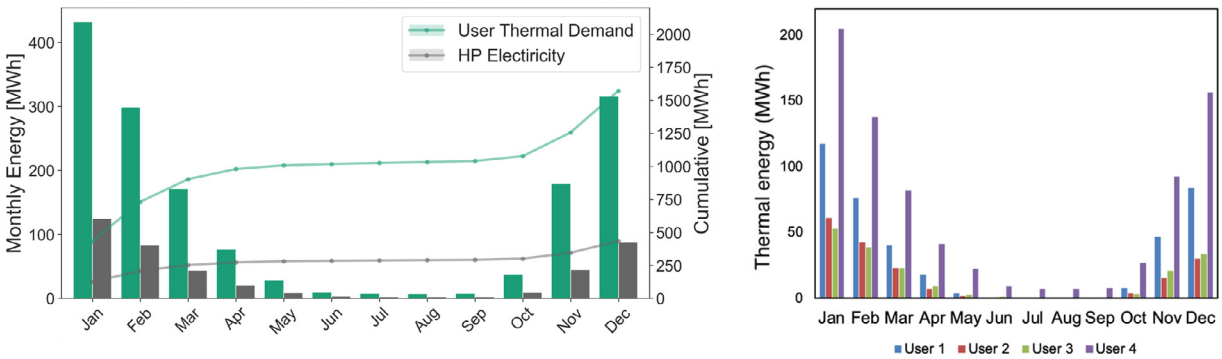

Fig. 2. (a) Monthly consumption retrieved from quasi bi-weekly measurements made in 2019. Monthly user thermal demand and HP electricity consumptions are measured at the condenser side of the HP. Curves show the cumulative energy; (b) Monthly thermal demand by user.

The monthly consumptions for 2019 are plotted in Fig. 2. In the left panel, the aggregate user consumptions are shown, distinguishing between heat demand on the user side (condenser side of HPs) and electricity demand of substations (HPs and user side circulation pumps). The right panel shows the split of the thermal demand among the users. It is observed that the users are of different sizes, but that the yearly distribution is similar for users apart from User 4, which includes a multifamily building and exhibits some SHW consumptions also during summer (while the other users have zero consumption in this season).

A more detailed analysis can be carried out using 2020 data, in which different temperature conditions in the network are reported in Fig. 3. The left panel shows the temperature distribution when source s_1 is active (refer to

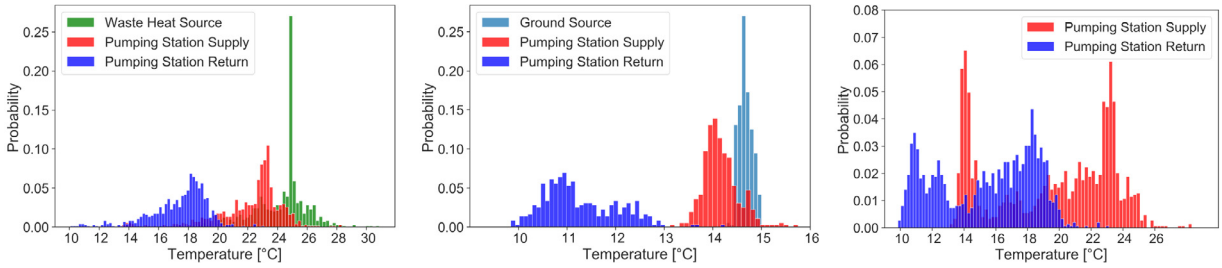

Fig. 3. Temperature distribution in different points of the network for different operating conditions. (a) Distribution when source s_1 is active; (b) Distribution when source s_2 is active; (c) Overall distribution at the pumping station. January–March 2020 data. See text for details.

Fig. 1 for positions): source s_1 temperature (green histogram) has a peak at about 25 °C, the supply temperature at position s_2 (where the pumping station and the aquifer wells are located; red histogram) has a peak at about 23 °C, the return temperature in the same position s_2 (blue histogram) has a peak at about 18 °C. Fig. 3(b) presents the situation when source s_2 (aquifer wells) is active: the green histogram is replaced by the light-blue histogram for the aquifer well temperature. All temperatures are clearly shifted to lower values. Finally, the right panel shows the overall temperature distributions at the pumping station (for all source cases). The supply-return temperature difference is of the order of 5 K, in reasonable agreement with the expected HP control.

Concerning the users' consumption behaviour, it is interesting to differentiate between summer and winter operations, since this corresponds to a distinction between SHW and SH operating conditions, respectively. This is also relevant because HPs operate according to a climatic curve, hence their COP depends on the ambient temperature and the type of demand. The left panel of Fig. 4 shows the typical distribution of SHW throughout the day. These profiles correspond to an average of few days of May 2020 (18th–23rd May 2020). All users have a much lower consumption during the night (zero for Users 1–3, including schools only). During the period from 06:00-23:00, a rather uniform random pattern can be seen instead. The observed SHW order of magnitude is expected to hold for most of the year, allowing to estimate the SH demand by subtracting the estimated SHW from the overall measured consumptions. The right panel of Fig. 4 focuses on SH demand and analyses their relationship with heating degree days (HDD): a reasonably linear behaviour is found (hourly data in the period January-March 2020 are used, where SH is dominant, and any error done for the SHW estimation is less relevant). This result suggests that a reasonable interpolation of the weekly/biweekly data of 2019 at a daily level can be done based on HDD. For an interpolation at an hourly level, one can also use the 2020 hourly data to retrieve a typical daily SH profile. Sample results for the different users are shown in Fig. 5(a), while Fig. 5(b) shows the aggregate behaviour retrieved from the pumping station data.

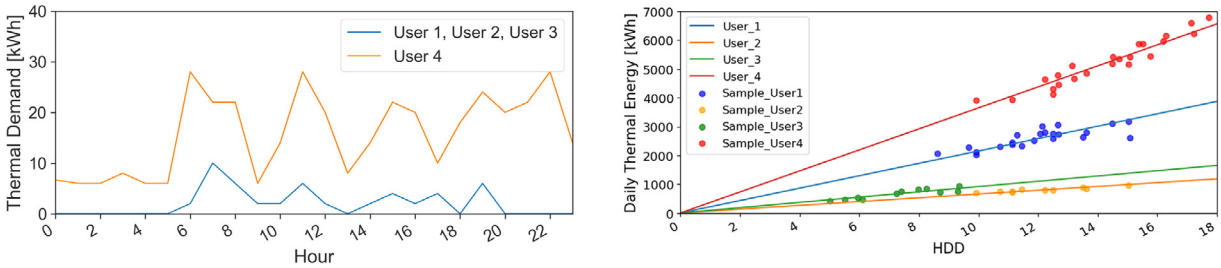

Fig. 4. (a) Sanitary hot water pattern of users 1 and 2; (b) Linear regression between thermal energy and heating degree days.

In general, winter plots are obtained from the retrieved data between 3rd Jan 2020–15th Mar 2020, with 747 hourly mean samples for s_1, and 359 for s_2.

As mentioned, the analysis of the 2020 data was used to interpolate 2019 data at an hourly level. Heat demands, measured in the user substations condenser side (E_{th,tot,h,u_i}), are the sum of the heat used for SHW preparation (E_{th,SHW,h,u_i}) and SH (E_{th,SH,h,u_i}). Summarizing, assuming that the daily total heat demand for SH is proportional

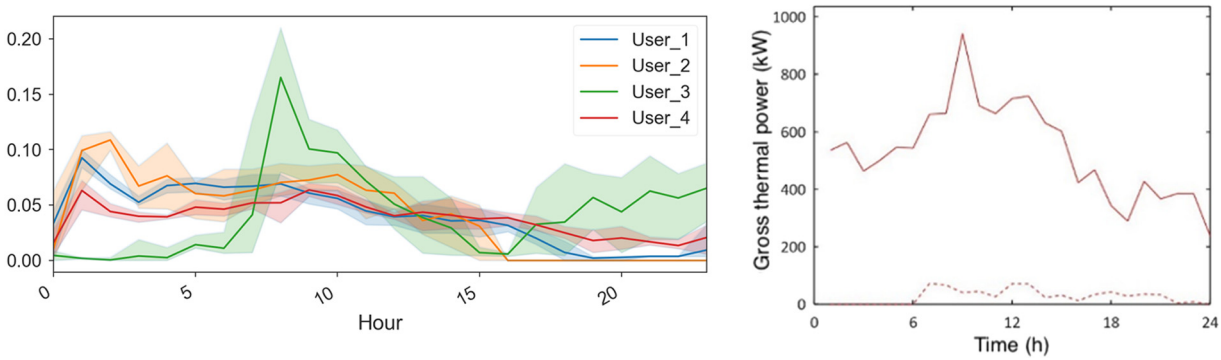

Fig. 5. February–March 2020 relative profile data.; (b) Aggregated monthly thermal load in 2019.

to HDD ($C_{user_i} \sim E_{th,SH,d,u_i}/HDD$), a proportionality constant (C_{u_i}) is estimated from linear regression applied to HDD and daily SH demand for the data collected in the period between Jan 2020 and Nov 2020. This allows us to estimate the daily SH heat demand for 2019, which is then distributed according to the users' hourly relative profiles that are shown in Fig. 5 (left). Relative profiles are generated from the data collected between February 2020 and March 2020, assuming that the schools were in normal operation and were not affected by Covid-19 related measures.

Overall network thermal losses ($E_{th,loss,ntw}$) were estimated by the difference between the total source thermal energy ($E_{th,WH} + E_{th,g}$) and the total thermal energy delivered to the evaporator side of user substations' HPs ($E_{th,HP,e}$). This was estimated from the difference between the thermal energy delivered on the HP condenser side ($E_{th,HP,c}$) and the HP electricity consumption ($E_{el,HP}$), assuming an adiabatic system. The efficiency (η_{ntw}) was then estimated as the ratio between the delivered energy to the users $E_{th,HP,e}$ and the total energy produced ($E_{th,WH} + E_{th,G}$). The timeframe considered was between Jan 22nd–31st of 2020, which was the only period of available data with all the necessary measurements.

3. Methodology

3.1. Neutral-temperature district heating network model

The structure of the NT-DHC network modelled in this case study considers the individual HPs located on the users' side as an aggregate load that draws the one-direction flow from the network supply pipe. The sources are connected in parallel, giving priority to the source with the highest temperature available, in this case, the steel plant. When this source is not available, the network is tempered down to the ground source temperature, assumed to provide continuous heat throughout the year.

The network supply temperature ($T_{net,s}$), assumed to be constant along all the network pipes, was estimated at each hour as a function of the available sources' temperature. The model considers the presence of various decentralized waste heat sources at different temperatures, however, in this case study the calculation is much simpler since only one waste heat plant is present, thus the estimated temperature supply is either (T_{s1}) when the plant is in operation, or the aquifer wells temperature (T_{s_2}) on the contrary.

The required temperature levels for SH (T_{SH}) provided to the users were calculated through a climatic curve. This temperature is bounded within the range of minimum ($T_{bldg,min}$) and maximum ($T_{bldg,max}$) limits depending on the outdoor temperature (T_{amb}) in this location. Since each user has its own SH setpoints, a weighted average proportional to their total thermal load was considered. Similarly, the minimum ($T_{amb,min}$) and maximum ($T_{amb,max}$) ambient temperature thresholds in which the SH system turns on or off were assumed according to the same proportion.

The determination of the ground temperature (T_g) for the estimation of thermal losses in the entire network was done according to textbook equations [14]. In this description of the ground behaviour, the ground responds in terms of daily or seasonal temperature cycles. Therefore, a daily approximation of the ambient temperature data available for the case study location was performed.

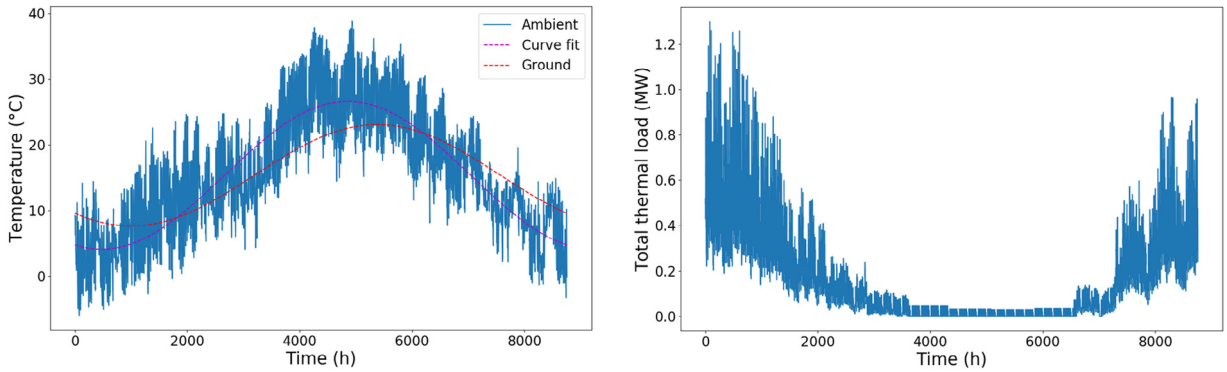

Fig. 6. (a) Input profiles for the model. Hourly ambient temperature (blue line), and ground temperature (red dashed line); (b) Aggregated thermal load profiles (condenser side of heat pumps (HPs)).

A curve that fits the data in a periodic manner is a typical problem in physics, in this case, it was applied a machine learning function in Python called "optimize-curve-fit" whose role is to apply non-linear least squares to fit a function of the type $T_{amb,fit}(t) = disp + amp \times \cos(t \times w - \emptyset)$ to some input data [15]. The fitted curve served as input for the ground temperature equation described in [16]. The resulting ambient temperature fitting and the consequent ground curve are presented in Fig. 6(a):

The HPs located on the users' substations work in parallel, with a variable operation depending on the load conditions. In this model, they are modelled in an aggregate manner, since the future application of this tool is to be able to reproduce fast estimations of potential new DH extensions with a larger number of users, under conditions where heating and cooling are supplied by the same network. Thus, Eq. (1) was selected from the literature [17] to represent a simplified physical understanding of the HPs pool performance. This COP function depends on the average temperature leaving the HPs' evaporators ($T_{e,o}$), which values vary depending on the available sources' temperatures; and the required temperature delivered on average to the users ($T_{c,o}$). In addition, a correction factor (η_{CF}) was included in this formula, to account for *phenomenological inefficiencies* of the modelled system due to other physical events beyond the scope of this analysis:

$$COP = 1 - \eta_m + \eta_m \times COP_C \tag{1}$$

$$COP_C = \frac{T_c}{Tc - T_e} \tag{2}$$

$$T_{c(e)} = T_{c,o(e,o)} \pm \Delta T_{HX} \tag{3}$$

$$COP_{CF} = \eta_{CF} \times COP \tag{4}$$

COP_C corresponds to the Carnot COP, a function of the condenser T_c and evaporator T_e refrigerant temperatures. These variables were determined through the external fluid inlet and outlet temperatures ($T_{e,o}$ and $T_{c,o}$, respectively), adjusted by a temperature drop at the HP condenser and evaporator (ΔT_{HX}), assumed to be the same in both cases. The compressor efficiency η_m varies due to multiple factors such as the HPs model, size, and operating conditions. It was possible to retrieve both η_m and ΔT_{HX} from the suppliers' machine datasheets by fitting equations (1) to (3) yielding the values of 53% and 2.15 K, respectively. Other effects – like thermal losses in substation pipes and buffers, pumping consumptions on the users' side, differences between datasheet and real HP performances, losses due to HP on/offs, climatic curve inaccuracies, and measurement uncertainty – are comprised in the aforementioned η_{CF} factor. In the absence of further information (e.g., a specific calibration, see below), the default value $\eta_{CF} = 1$ can be used.

Thermal losses on the entire network ($E_{loss,net}$) were calculated as a function of pipe lengths and diameters, pipe insulation properties given by an average overall heat exchange coefficient (U_{avg}), network supply ($T_{net,s}$) and return temperatures ($T_{net,r} = T_{net,s} - \Delta T_{evap}$), and ground temperature (T_g). The supply-return network temperature difference (ΔT_{evap}) was assumed to be at a constant 5 K due to the heat pumps' control settings, however, a sensitivity analysis in the range from 3–5 °C is performed in alignment with the monitoring values presented in

Fig. 3. As the network geometry and pipes' characteristics were known, all the material properties were obtained from datasheets. Similarly, as in the case of the COP estimation, a correction factor U_{CF} was introduced, with the aim of finding the best match with real thermal losses measurements. The default value before calibration is again $U_{CF} = 1$.

$$E_{loss,net} = U_{avg} \times \left[\left(T_{net,s} - T_g\right) + \left(T_{net,r} - T_g\right)\right] \tag{5}$$

$$E_{loss,CF} = U_{CF} \times E_{loss,net} \tag{6}$$

3.2. Key performance indicators

The experimental data available was typically measured on a bi-weekly basis, therefore the key performance indicators (KPIs) selected for the comparison were determined by integrating the energy data on a monthly and annual fashion. The energy carried by the network to the HPs evaporator side ($E_{th,HP,e}$), assuming an adiabatic system, was estimated as the difference between the heat delivered to the users ($E_{th,HP,c}$) and the HPs electric consumptions ($E_{el,HP}$). In addition, the seasonal COP (SCOP) is calculated as the ratio between the annual thermal energy on the condenser side and the yearly electric energy consumed at the user substation (SCOP $= E_{th,HP,c}/E_{el,HP}$), this represents the performance of HPs only. The SPF, on the other hand, represents the overall efficiency of the system. It includes the electricity used by the HPs and the electric consumption of the network pumps ($E_{el,pump}$). Finally, $E_{el,pump}$was estimated as a function of the network flow rates and the pump capacity in each of the network circuits (primary and secondary loops, and the aquifer wells circuit). Besides the yearly analysis, it was also of interest to assess these indicators on a monthly basis to evaluate the seasonality effects.

The correction factor η_{CF} was evaluated to find the best fit with the real data. Several simulations were performed, and the modelled parameters were compared according to two metrics: an accuracy metric with respect to the SCOP, represented by Eq. (7), and the mean squared error (MSE) of the monthly COP estimates of the model according to Eq. (8); where $f_i\,(COP)$ is a vector of residuals, $m\,(COP_i)$ is the COP predicted by the model in month i, and COP_i is the observed value.

$$Accuracy = (SCOP_{real} - SCOP_{corr})/SCOP_{real} \tag{7}$$

$$MSE = \frac{1}{N}\sum_{i=1}^{N} f_i(COP)^2 \tag{8}$$

$$f_i\,(COP) = m\,(COP_i) - COP_i \tag{9}$$

4. Results

4.1. Sensitivity analysis

Temperature data on the network side of the users' substations were not available for this analysis. However, they could be estimated from the monitoring data at the pumping station. The most relevant case is when source s_1 is active (since this occurs for more than 80% of the time), where the estimate yields $T_{s_1} = 22$ °C and $\Delta T_{evap} = 4$ °C for the temperature at the HP inlet and the supply-return temperature difference, respectively. With these conditions, the hourly COP values are distributed in the range 4–5.6. In both cases, the best performance is obtained in climatic conditions where the outdoor air temperature is within the range of 7 to 20 °C and when the maximum temperature supplied to the users is below 50 °C. Since an uncertainty of a few degrees remains on T_{s_1} and ΔT_{evap}, a sensitivity analysis was performed on these values, varying T_{s_1} in the range 18–22 °C and ΔT_{evap} in the range 3–5 °C. It was observed that the hourly COP values are barely affected by these changes, i.e., less than 5%. The values T_{s_1} = 22 °C and $\Delta T_{evap} = 4$ °C are hereafter considered the reference values for a "default model" simulation, i.e., a simulation based on the real inputs but no adjustment of the correction factors η_{CF} and U_{CF} (see Fig. 7).

4.2. Calibration

The available monitoring data was aggregated in a monthly fashion, to compare with the predicted COP and SPF. Table 1 presents the accuracy of the model and the MSE calculated when using different correction factors

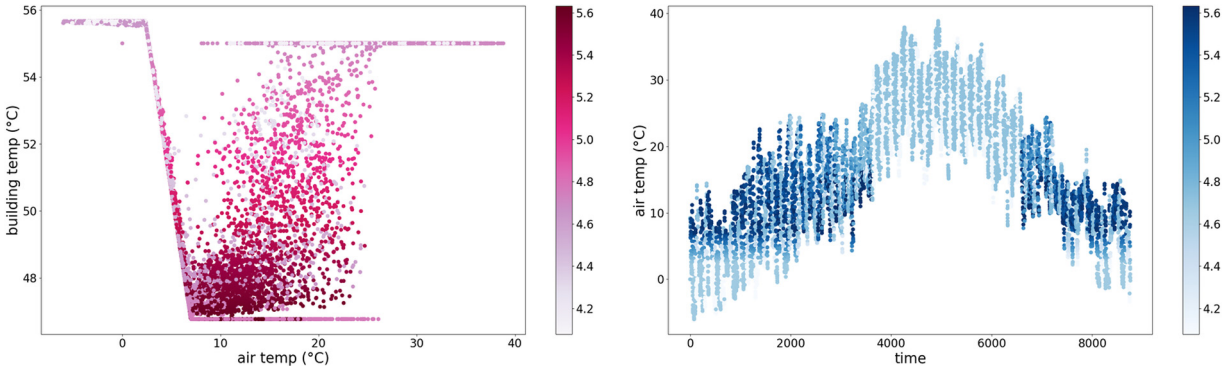

Fig. 7. COP performance map. The colours represent hourly values in the range of the colour bars. (a) Effect of the climatic curve implemented in the model; (b). Climate influence in the COP. The points in dark blue indicate a better performance in spring and autumn seasons. (For interpretation of the references to colour in this figure legend, the reader is referred to the web version of this article.)

(η_{CF}) according to Eq. (4). It is observed that the best fit is obtained for $\eta_{CF} = 75\%$. This means that the overall substation inefficiencies are on the order of 25%. While a 15% of performance losses can be expected, this is a rather high correction, which might be due not only to the actual substations' performance but also to the various approximations of the model (see Fig. 8).

For the thermal loss correction factor U_{CF}, a calibration was performed using selected data (Jan 22nd to Jan 31st). The total measured losses in this period are 26 MWh, significantly lower than the default prediction, yielding $U_{CF} = 37\%$. This large discrepancy is related to a shortcoming in the "default" calculations: the thermal losses are estimated assuming an undisturbed ground temperature at the pipe wall. While this is appropriate for insulated pipes (where insulation constitutes most of the thermal resistance) and can be used for conventional district heating modelling, it fails in the case of non-insulated plastic pipes. It was found that the observed U_{CF} corresponds to the case in which the undisturbed ground temperature is reached at about 0.25 m from the pipe wall (this is the equivalent of assuming the existence of an effective ground insulation layer of 0.25 m around uninsulated pipes). Finally, the results of the annual analysis show a reasonable agreement between the main KPIs of the model and the data. (See Table 2).

Table 1. Sensitivity analysis of correction factor applied to COP function.

η_{CF}	SCOP	Accuracy (%)	MSE
74	3.57	1.43	0.00268
75	3.62	0.0499	3.26×10^{-6}
76	3.67	1.33	0.00232

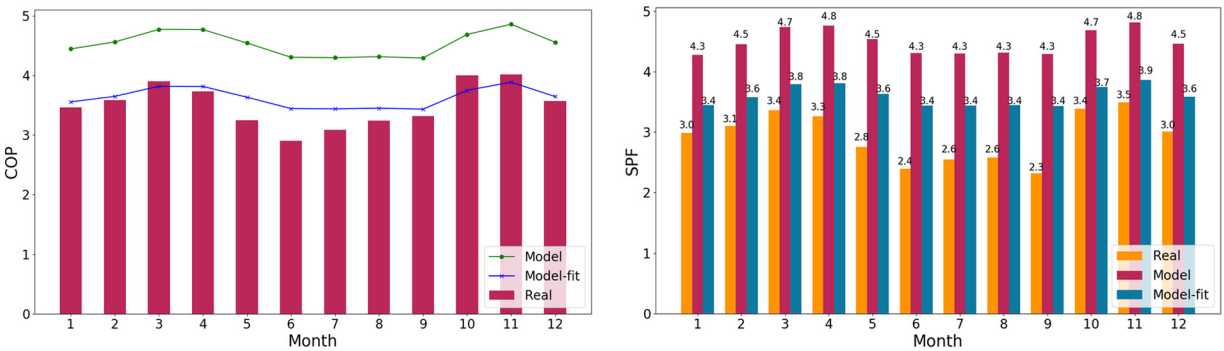

Fig. 8. COP and SPF outputs before and after the application of the correction factor that better fits the experimental data.

Table 2. Yearly performance and energy balances comparison.

Quantity	Unit	Model		Monitoring data	%Diff
$E_{th,HP,c}$	MWh/y			1557.63	
T_{S_1}	°C	20	22	24.28 ± 1.9	
T_{aq}	°C	15.33		14.67 ± 0.14	3.79–55
SCOP	arb. u.	3.61	3.64	3.62	0.27–0.55
SPF	arb. u.	3.16	3.17	3.11	1.61–2.57
$E_{th,HP,e}$	MWh/y	1125.94	1127.61	1128.9	0.11–0.26
$E_{el,HP}$	MWh/y	431.69	427.54	433.5	0.42–1.37
$E_{el,pump}$	MWh/y	49.66	50.47	65.2	22.59–23.83

5. Conclusions

In this contribution, the performance of a real neutral-temperature DH network is analysed and compared with a lumped model suitable for scenario analysis. The network relies on source temperatures between 15 and 25 °C and exhibits an SPF of about 3.11. Large parts of the network pipes are uninsulated, nevertheless yielding thermal losses of the order of 30%. Electric pumping consumptions are of the order of 4% of the users' thermal consumptions. The approximated model provides proper order of magnitudes for these values even using simplified default estimates. However, to get a good agreement (a few percent of the difference in the most important indicators), a calibration of two simple phenomenological coefficients is required. The use of an aggregate approach seems satisfactory for such a simple network (main deviations between non-calibrated model and real data can be explained with physical details not related to the differences between single users). The main value of such an approximate aggregated model is to offer a quick tool for scenario analysis (the model also includes economic estimates), a needed application for this innovative neutral-temperature network strongly coupling thermal and electric consumptions.

Declaration of competing interest

The authors declare that they have no known competing financial interests or personal relationships that could have appeared to influence the work reported in this paper.

Acknowledgements

The present work is part of the LIFE4HeatRecovery project, funded by the LIFE Programme of the European Union under contract number LIFE17 CCM/IT/000085. The authors gratefully acknowledge the availability of Manuel Piatti and Federico Orizio by Cogeme for sharing information and useful discussions about the Ospitaletto network.

References

[1] Yang X, Svendsen S. Ultra-low temperature district heating system with central heat pump and local boosters for low-heat-density area: Analyses on a real case in Denmark. Energy 2018;159:243–51. http://dx.doi.org/10.1016/j.energy.2018.06.068.
[2] Lund H, et al. 4th generation district heating (4GDH): Integrating smart thermal grids into future sustainable energy systems. Energy 2014;68:1–11. http://dx.doi.org/10.1016/j.energy.2014.02.089.
[3] Averfalk H, Werner S. Economic benefits of fourth generation district heating. Energy 2020;193:116727. http://dx.doi.org/10.1016/j.energy.2019.116727.
[4] Lund H, et al. The status of 4th generation district heating: Research and results. Energy 2018;164:147–59. http://dx.doi.org/10.1016/j.energy.2018.08.206.
[5] Østergaard PA, Andersen AN. Economic feasibility of booster heat pumps in heat pump-based district heating systems. Energy 2018;155:921–9. http://dx.doi.org/10.1016/j.energy.2018.05.076.
[6] Termis engineering | schneider electric. 2020, https://www.se.com/my/en/product-range-presentation/61613-termis-engineering/ (accessed Nov. 16, 2020).
[7] Thermos tool. 2016, THERMOS H2020 project https://www.thermos-project.eu/thermos-tool/thermos-tool/ (accessed Nov. 16, 2020).
[8] The PLANHEAT tool. 2019, PLANHEAT project https://planheat.eu/the-planheat-tool.
[9] EnergyPLAN. 2020, Department of Development and Planning, Aalborg University https://www.energyplan.eu/.
[10] LEAP. 2020, https://leap.sei.org/default.asp (accessed Nov. 16, 2020).
[11] Artelys Crystal City. 2021, Artelys https://www.artelys.com/crystal/city/.
[12] METIS. 2019, European Commission https://ec.europa.eu/energy/data-analysis/energy-modelling/metis_en (accessed Mar. 26, 2021).

[13] Bava F. FLEXYNETS D6.11, Pre-design support tool.
[14] Banks D. An Introduction to Thermogeology: Ground Source Heating and Cooling. John Wiley & Sons; 2012.
[15] Martínez-Barbosa Carmen, Celis-Gil José. Fitting cosine(Sine) functions with machine learning in python. 2020, Medium https://towardsdatascience.com/fitting-cosine-sine-functions-with-machine-learning-in-python-610605d9b057 (accessed Mar. 25, 2021).
[16] Calixto S, Cozzini M, Manzolini G. Modelling of an existing neutral temperature district heating network: Detailed and approximate approaches. Energies 2021;14(2). http://dx.doi.org/10.3390/en14020379, Art. (2).
[17] Grassi W. Heat Pumps: Fundamentals and Applications. Springer; 2018.